Journal of Hazardous Materials 469 (2024) 134084

Contents lists available at ScienceDirect

Journal of Hazardous Materials

journal homepage: www.elsevier.com/locate/jhazmat

Research Paper

Establishment of a system to analyze effects of airborne ultra-fine particulate matter from brake wear on plants under realistic exposure conditions

Ludwig Richtmann [a], Thorsten Opel [b], Marina Maier [c], Nico Langhof [b], Stephan Clemens [a,*]

[a] Plant Physiology, University of Bayreuth, 95447 Bayreuth, Germany
[b] Ceramic Materials Engineering, University of Bayreuth, 95447 Bayreuth, Germany
[c] Bavarian State Office for the Environment, 86179 Augsburg

HIGHLIGHTS

- A system for airborne exposure to ultrafine particles (UFP) from brake dust was established.
- Particle concentration and elemental composition were determined with single particle ICP-MS and ELPI+.
- UFP quantification after outdoor exposure was done to set laboratory exposure in a realistic context.
- Physiological effects after controlled exposure of the model A. thaliana were characterized with RNA sequencing.

GRAPHICAL ABSTRACT

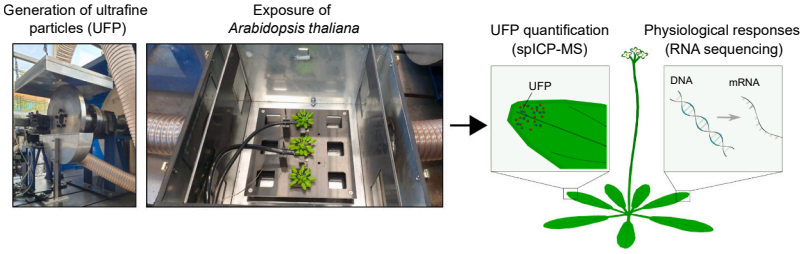

ARTICLE INFO

Keywords:
Air pollution
Nanoparticle emission
Nanoparticle toxicity
Non-exhaust emissions
spICP-MS
RNA sequencing

ABSTRACT

Research on airborne ultrafine particles (UFP) is driven by an increasing awareness of their potential effects on human health and on ecosystems. Brake wear is an important UFP source releasing largely metallic and potentially hazardous emissions. UFP uptake into plant tissues could mediate entry into food webs. Still, the effects of these particles on plants have barely been studied, especially in a realistic setting with aerial exposure. In this study, we established a system designed to mimic airborne exposure to ultrafine brake dust particles and performed experiments with the model species *Arabidopsis thaliana*. Using advanced analytical methods, we characterized the conditions in our exposure experiments. A comparison with data we obtained on UFP release at different outdoor stations showed that our controlled exposures are within the same order of magnitude regarding UFP deposition on plants at a traffic-heavy site. In order to assess the physiological implications of exposure to brake derived-particles we generated transcriptomic data with RNA sequencing. The UFP treatment led to diverse changes in gene expression, including the deregulation of genes involved in Fe and Cu homeostasis. This suggests a major contribution of metallic UFPs to the elicitation of physiological responses by brake wear derived emissions.

* Correspondence to: Department of Plant Physiology, University of Bayreuth, Universitätsstraße 30, 95447 Bayreuth, Germany.
E-mail address: stephan.clemens@uni-bayreuth.de (S. Clemens).

https://doi.org/10.1016/j.jhazmat.2024.134084
Received 21 December 2023; Received in revised form 20 February 2024; Accepted 18 March 2024
Available online 19 March 2024

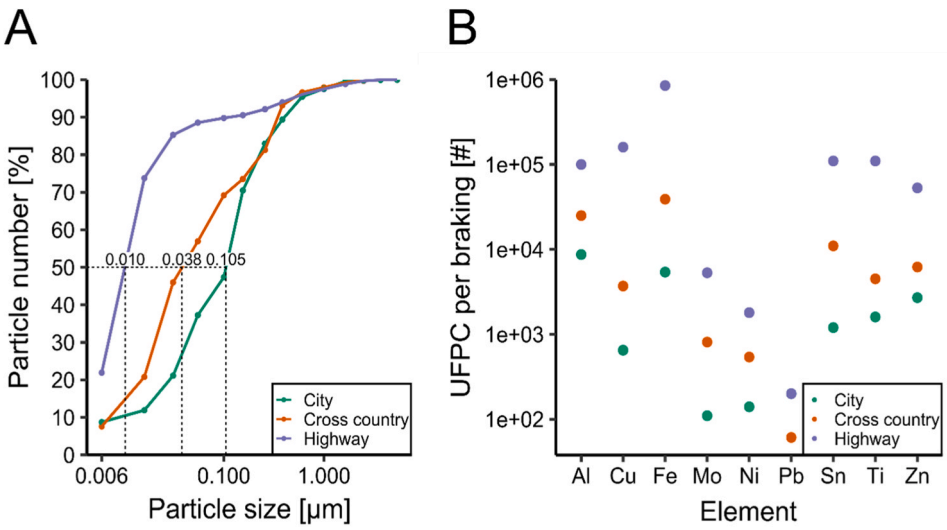

Fig. 1. Particle emission at the brake test bench. A: Cumulative curve of particle number versus particle size for three different use cases. Particle collection and size distribution measurement were done with 20 brakings using an impactor (ELPI+, DEKATI). Dashed lines indicate the D_{50} values for the respective use cases. B: Number of UFPC per braking for the different use cases. Particles of 20 brakings were collected using an impactor (ELPI+, DEKATI) and the ultrafine fractions were analyzed with spICP-MS.

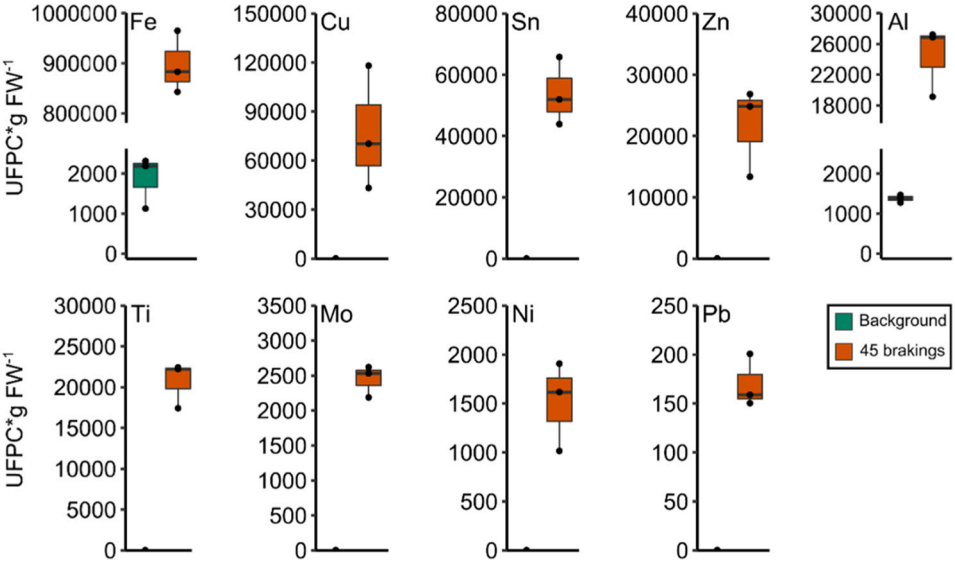

Fig. 2. Quantification of UFP deposition on plant leaves after controlled exposure. 4–5-week-old *A. thaliana* plants were subjected to 45 brakings (highway use case, 2 MPa) or to the background exposure (resuspended particles in the pipes and exposure chamber). Particles were extracted and analyzed with spICP-MS. Data from three independent exposure experiments are shown as ultrafine particle constituents (UFPC) per gram fresh weight (FW).

1. Introduction

The economic growth and development of human societies has been accompanied by the emergence of environmental challenges [1]. Among these, air pollution, especially from particulate matter (PM), stands out as a major – and growing - concern [2]. PM pollution in urban areas is ubiquitous, as evidenced by a recent WHO report indicating that the majority of settlements across the world displayed annual mean PM values that exceed safety limits [3].

PM is categorized into coarse (PM_{10}, 2.5 µm< d_p <10 µm), fine ($PM_{2.5}$, d_p <2.5 µm), and ultrafine ($PM_{0.1}$, d_p <0.1 µm) fractions [4]. Ultrafine particles (UFP) possess negligible weight and often show inhomogeneous spatial distribution, resulting in their minimal contribution to total $PM_{2.5}$ or PM_{10} mass concentrations [5]. Consequently, conventional PM monitoring strategies that rely on interpreting PM_{10} and $PM_{2.5}$ mass concentrations are prone to misinterpretation, i.e. underestimating the actual presence of UFP. Instead, the use of particle number concentration (PNC) or particle number size distribution (PNSD) have been shown to be more informative for assessing UFP pollution [5,6].

UFP are released into the atmosphere from various sources, both natural and anthropogenic. In particular, studies have highlighted the significant role of road traffic in UFP emissions [7–9]. While exhaust emissions from sources like diesel combustion remain a major contributor, non-exhaust emissions such as brake and tire dust contribute to UFP emissions as well [10]. Particles from brake wear in particular account for the majority of non-exhaust emissions arising from traffic [11].

In recent years, UFP have attracted significant attention in light of several studies establishing their detrimental effects on human health [12,13]. Because of their high surface to mass ratio, UFP have a high capacity to adsorb toxic trace metals and organic chemicals [14]. Additionally, owing to their potential to pass primary airway defenses

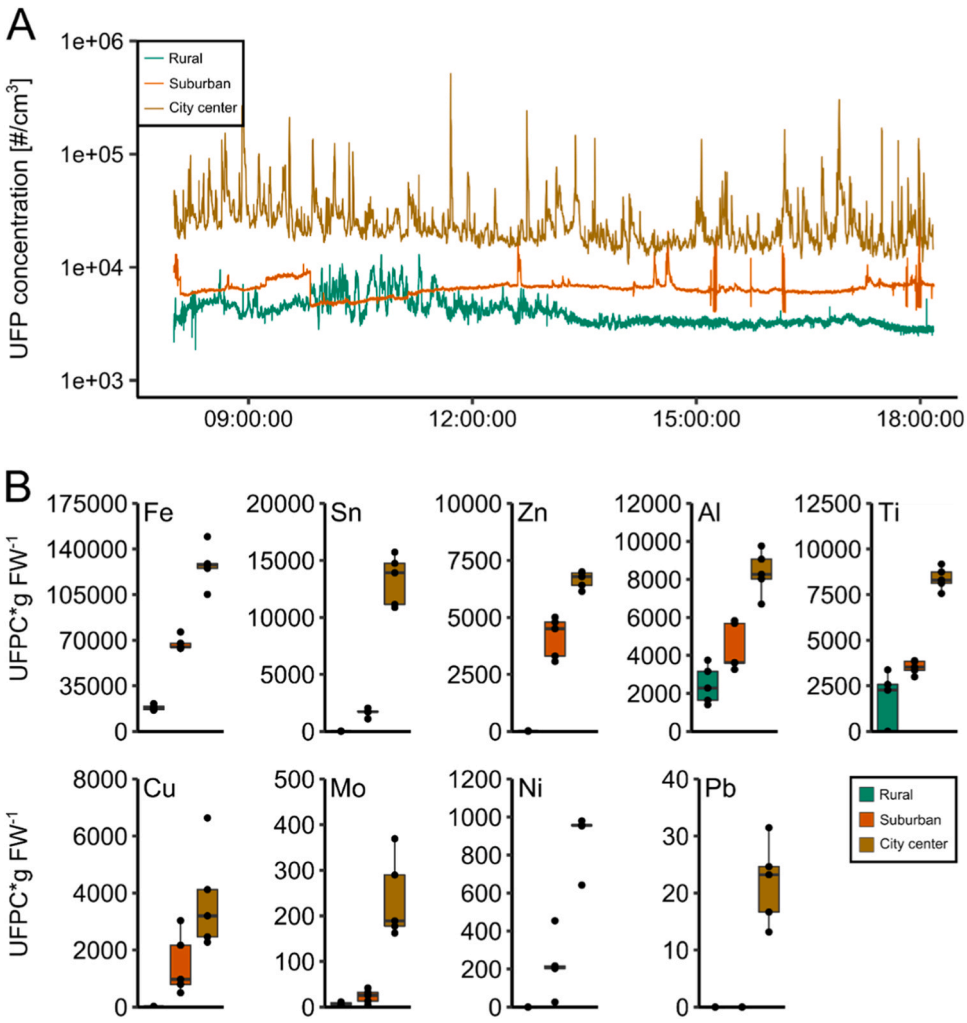

Fig. 3. UFP concentration in the field and UFP deposition on plant leaves after outdoor exposure. A: ELPI+ -measurement of UFP (6–100 nm) concentration during one day at three locations with varying traffic volume**.** B: 4–5-week-old *A. thaliana* plants were placed for 14 days at the locations from A. Particles were extracted from rosettes and measured with spICP-MS. Data from one exposure experiment and five plants per location. Data are shown as ultrafine particles (UFP) per gram fresh weight (FW).

and achieve systemic translocation, UFP may inflict harm beyond the respiratory system [7].

As the focus on UFPs intensifies, it becomes crucial to investigate their impact not only on human health but also on the broader environment, including plants. Many years of research have improved our understanding of metal phytotoxicity [15], but very little attention has to date been devoted to airborne metallic particles. Given a small enough size, they possibly may enter plant tissues through stomata, the pores present on leaf surfaces responsible for gas exchange [16,17]. Together with the presence of high levels of Cu and other elements like Sn and Pb in brake linings [18], this makes UFP from brake wear potentially harmful to plants. In addition, brake linings contain a variety of organic components, that may cause toxic effects in plants as well [18]. Exploring the effects of brake wear UFP on plants not only fills a gap in the assessment of potentially phytotoxic atmospheric particles but also addresses the importance of understanding the broader ecological implications of UFP pollution. Furthermore, the deposition on surfaces or the uptake into plant tissues represents a potential entry point for UFP into food webs and human food, possibly adding to the already dominant contribution of plant-derived food to non-occupational metal exposure [19]. This aspect may become even more relevant with the budding interest in urban farming [20].

In this study, we present the establishment of controlled airborne exposure experiments with brake wear-derived UFP using an exposure chamber connected to a brake dynamometer. The experiments were conducted with the model species *Arabidopsis thaliana,* which has been widely used in stress physiological research because of its annotated genome and decades of mutant analysis which have led to a profound functional understanding of a vast number of genes [21]. Applying state of the art methods such as spICP-MS and ELPI+, we precisely characterized the exposure conditions. We contextualize our experimental results by presenting a quantitative assessment of UFP deposition on leaves after outdoor exposure at three locations that we analyzed with regards to aerial particle concentration. Furthermore, we show an analysis of the transcriptome response to brake-wear particles by RNA sequencing and the identification of responsive pathways and processes.

2. Material and methods

2.1. Plant material and growth conditions

Arabidopsis thaliana (Col-0) plants were grown for 4–5 weeks on standard potting-soil (consisting of 3 parts potting soil, 3 parts standard soil and 1 part vermiculite) in short day conditions (8 h 80 μE light/16 h darkness) at 25 °C using 5 x 5 x 5.5 cm pots.

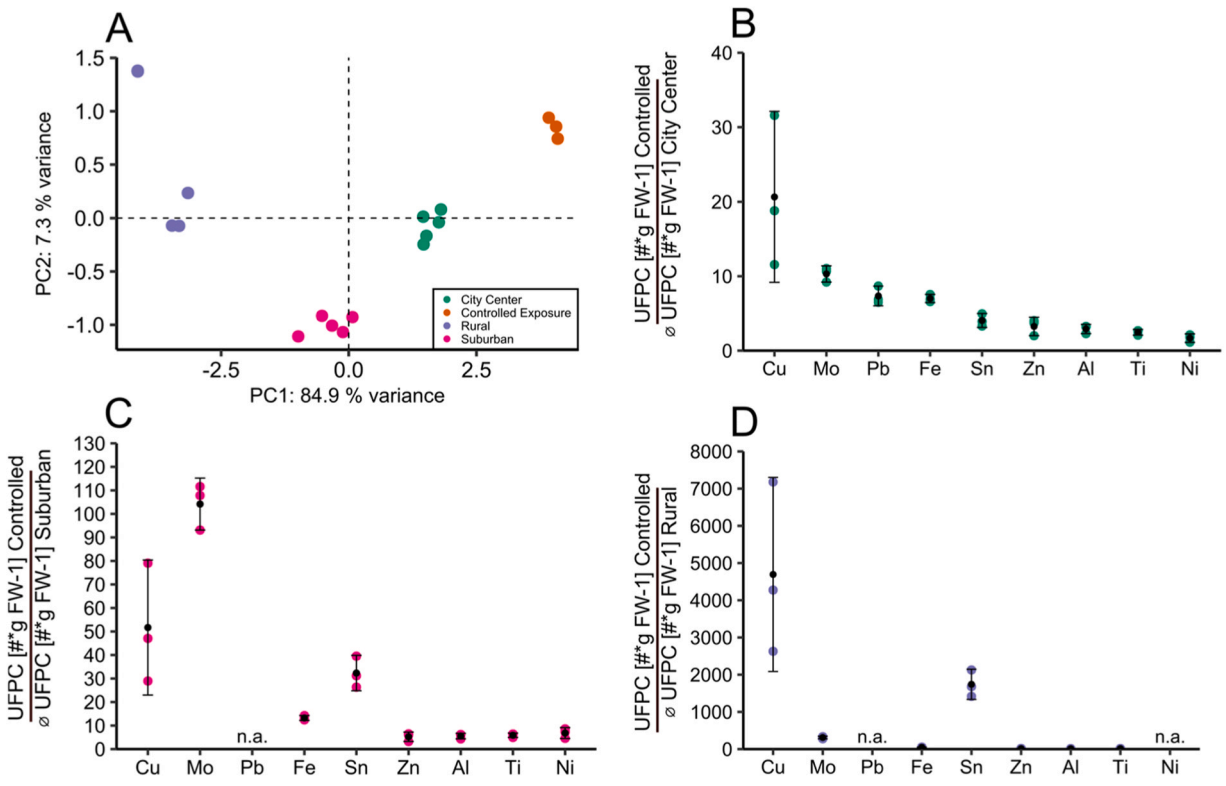

Fig. 4. spICP-MS results for outdoor exposed plants compared to plants subjected to controlled exposure. A: Distribution of UFPC of outdoor exposed plants and plants exposed to wear from 45 controlled brakings according to PC1 and PC2. The percentage of variance explained for each principal component is reported. B-D: UFPC contents after controlled exposure compared to the mean of each outdoor exposure location. Graphs display the mean +/- standard deviation.

2.2. Controlled UFP generation and exposure

For the generation of UFP, a unique, self-built dynamometer brake test stand was used (Fig. S1**).** The brake test stand involves an 800 kg fly wheel, a 45 kW electric motor, a flange with adapters for different brake discs and a pneumatically actuated brake calliper. The brake discs were not internally ventilated and had an outer diameter of 450 mm and a thickness of 356 mm and were manufactured out of grey cast iron (GJL-150). The brake pads used were conventional LowMet brake pads supplied by TMD Friction GmbH (Leverkusen, Germany) with a size of 30 x 30 x 10 mm^3 .

During testing, they were subjected to braking pressures of 2 and 3 MPa. Each test run involved up to 45 repeated brakings from a maximum start sliding velocity of 20 $m*s^{-1}$ to full stop, which translates to a braking energy of approximately 0.6 MJ. For all test runs, the friction radius was kept constant at 205 mm.

To perform controlled and reproducible exposure experiments with plants, we integrated an exposition chamber into the exhaust system of the dynamometer test rig (Fig. S1). A special specimen mount was designed, so that a reproducible positioning of the plants as well as a reproducible measuring position for the aerosol measurements could be achieved (Fig. S1, B) Emissions of three distinct use-cases with different starting sliding velocities and resulting braking energies were investigated. The use-cases represent a city braking maneuver (v_{start} = 5 $m*s^{-1}$; E_{brake} ≈ 0.04 MJ), a cross-country road braking maneuver (v_{start} = 10 $m*s^{-1}$; E_{brake} ≈ 0.15 MJ) and a highway braking maneuver (v_{start} = 20 $m*s^{-1}$; E_{brake} ≈ 0.59 MJ). The wear behavior of the chosen friction pairing was characterized by measuring the wear coefficient k after 20 successive brake applications at the respective use-cases and brake pressures of 2 MPa and 3 MPa.

In order to reduce the amount of mechanical stress for plants and ensure better dispersion of particles, two windshields were installed at the entry and exit of the chamber (Fig. S1). Due to the heat development of the friction pairing, the wear of 45 full-stop highway brakings was delivered in an alternating nesting with the background exposure (Fig. S2, A). In this way, the exposure of the plants to temperatures above 30 °C was avoided (Fig. S2, B).

2.3. Analysis of aerial UFP concentration with ELPI+

Particles < 100 nm were sampled with an electrical low-pressure impactor (ELPI+) (Dekati Ltd., Kangasala, Finland). ELPI+ is a real-time particle spectrometer that consists of 15 stages, including 14 impactor stages and a filter stage. The device separates and measures particles from 6 to 10 000 nm. ELPI+ was operated according to the manufacturer's recommendations by setting the flow rate of sampling air to 10 $l*min^{-1}$ and capturing particles on polycarbonate foils (25 mm in diameter, Whatman Nuclepore, GE Healthcare, USA). Before commencing the sampling process, we applied DS-515 collection substrate spray (Dekati Ltd., Kangasala, Finland) to minimize particle bouncing. ELPI+ was used with the DD 603 dryer (Dekati Ltd., Kangasala, Finland) in order to eliminate moisture from the sample. Samples were collected between 8 a.m. and 6 p.m.

2.4. spICP-MS measurement of particles collected with ELPI+

Before the analysis, polycarbonate foils with UFP were put in 15 ml micelle-forming tenside solution of 0.25% (w/w) Triton-X-114 (VWR International, Belgium), shaken for 3 min and treated in an ultrasonic bath for 10 s to ensure sample homogeneity. Dispersed particles were analyzed using spICP-MS as described below. To validate the measurement method, the collection foils were prepared with monodisperse gold nanoparticles (NIST RM 8013, 60 nm, 1.5 $*10^7$ particles/foil) as reference material before sampling. Since these particles hardly occur in nature and in brake pads, they can be used as an internal standard for quality assurance of the measurement process. The recovery rate was

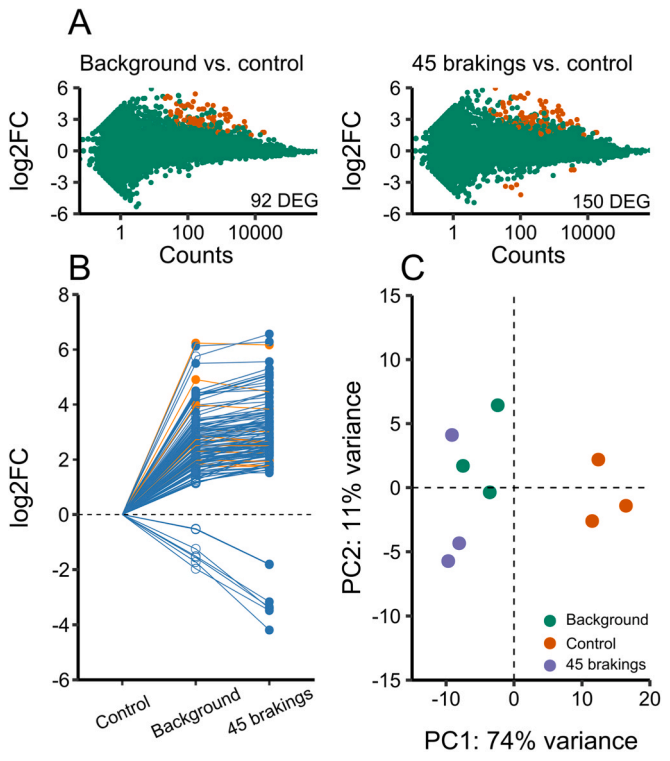

Fig. 5. RNA sequencing of *A. thaliana* subjected to aerial exposure with brake wear particles. A: MA plots showing significant (orange) DEG when comparing gene expression in background exposed plants versus controls or plants exposed to 45 brakings with controls. Green dots represent genes not differentially expressed. Significance of DEG was identified with DESeq2 (lfcThreshold =1, $p_{adj} \leq 0.05$. B: Curve-array showing the expression of UFP-responsive DEG over the different sample groups. Genes showing a progressive increment/decrement are labeled in blue, genes without increment/decrement are labeled orange. Filled circles indicate significant differential expression compared to the outside control as identified with DESeq2, non-filled circles indicate non-significant changes. C: Distribution of inside/outside control samples and samples of plants subjected to 45 brakings according to PC1 and PC2. The percentage of variance explained for each principal component is reported.

85–87%.

2.5. Outdoor exposure of Arabidopsis thaliana

Prior to outdoor exposure, plants were grown as described above (Section 2.1). Rosette stage plants (4–5 weeks old) were placed from 19.09.2022–04.10.2022 at a rural location (Coordinates: 47.96875, 11.22017), a suburban location (Coordinates: 48.32601, 10.90305) and an inner-city location (48.37027, 10.89628) on ground level. At least five plants were placed at each location. Plants were inspected every 4 days and watered if necessary.

2.6. Extraction of particles from plant material

UFP extraction from leaves of *A. thaliana* was done according to a modification of the methanol-based extraction from [22]. Briefly, frozen leaves were put in a 50 ml centrifuge tube containing 20 ml of 10 mM CAPSO (3-(cyclohexylamino)−2-hydroxypropane-1-sulfonic acid) solution (pH 9 adjusted with KOH). The sample was then homogenized with a Witeg HG-15A homogenizer (Witeg, Wertheim, Germany) and probe sonicated for 3 min in intervals of 10 s with a Bandelin Sonopuls HD 200 (Bandelin, Berlin, Germany). Of each sample, three replicate aliquots were extracted by transferring 500 µl of the suspension to a new 15 ml tube before adding 3.75 ml of 50 % (v/v) methanol. The solution was placed on an orbital shaker (150 rpm, 1 h) before adding 1.25 ml of 1 % (v/v) Tween 80 and the repetition of the ultrasonication step. Samples were filtered with a nylon syringe (1 µm pore size) filter and diluted 10-fold with ultrapure water for single particle analysis.

2.7. spICP-MS

Inductively coupled single-particle plasma mass spectrometry (8900 triple-quadrupole ICP-MS, Agilent Technologies, Tokyo, Japan) was used for the quantification of inorganic particles < 100 nm. The sample introduction system included a concentric glass nebulizer, a quartz spray chamber, a quartz torch with a 1.5 mm injector and standard nickel cones.

The dwell time used was 100 µs for an acquisition time of 60–300 s. Transport efficiency was determined with gold nanoparticles (NIST RM 8013, 60 nm, 2.9 $*10^{13} \pm 3$ % particles$*l^{-1}$, Gaithersburg, MD, USA) following a previously approved procedure [23]. Signal sensitivity was calibrated with a multielement standard solution (1000 mg$*l^{-1}$ in 6% HNO_3; Merck, Germany) at a concentration of 1 µg$*l^{-1}$. Particles were measured in the concentration range of $2 * 10^3$ to 10^8 particles$*l^{-1}$ [24, 25]. The ultrafine Pb particles were additionally determined using cloud point extraction [26] in conjunction with spICP-MS. Data acquisition of the metal-based particles was performed with the software MassHunter Version 4.6. Principal component analysis of the spICP-MS data was done with the R packages “factoextra” and “FactoMineR”. Prior to the analysis, an integer of 1 was added and the data were log2-transformed.

2.8. Scanning electron microscopy

Directly after exposing plants to brake wear particles, leaves were freeze-dried for 4 h. Furthermore, samples were covered with a 2 nm Pt-layer using a Leica EM ACE600 sputter-coater (Leica, Germany). Scanning electron microscopy was done with a JSM-IT-500 microscope (JEOL, Japan).

2.9. RNA sequencing

24 h post-exposure to brake wear particles, *A. thaliana* rosettes were frozen in liquid nitrogen. For every sample, the rosettes of 6 separate plants were pooled. RNA extraction, library preparation, sequencing and data processing were done as described in [27]. Differential expression analysis, principal component analysis and extraction of normalized counts for further analysis was done with DESeq2 (lfcThreshold =1, $p_{adj} \leq 0.05$) [28]. GO-overrepresentation analysis was done with PANTHER (http://www.pantherdb.org/), using Fisher’s exact test and Bonferroni correction.

3. Results and discussion

3.1. Development of controlled exposure experiments

Dynamometer-based brake-particle generation and characterization have been conducted in the past and were highlighted as the most efficient and reliable approach (reviewed in [29]). We assessed the tribological characteristics of our brake system using different brake pressures and E_{kin} represented by three use cases. We determined an increase in wear coefficient **k** with E_{kin} and found that **k** is consistently higher at a brake pressure of 2 MPa compared to 3 MPa, which is expected to result in higher particle emission (Table S1). For all three use cases, we measured particle size and number distribution in the chamber at 2 MPa with an ELPI+ . In a cumulative analysis of particle number versus particle size, we found that the highway braking leads to the highest proportion of UFP (D_{50} = 0.01 µm), followed by the cross-country road braking (D_{50} = 0.038 µm) and the city braking (D_{50} = 0.105 µm) (Fig. 1A). Our results align with previous work, in which a similar trend towards smaller particles with increasing E_{kin} was observed [30].

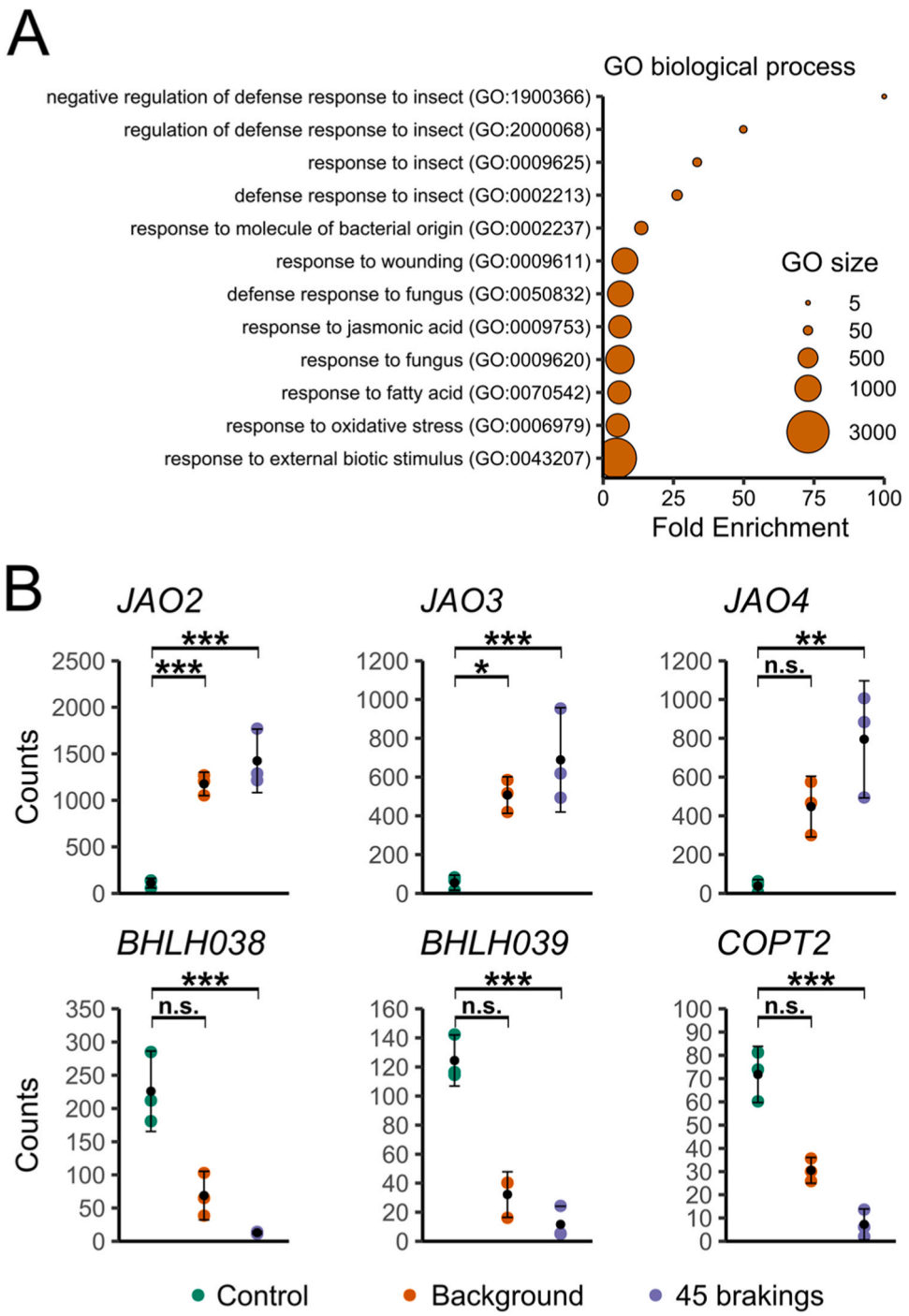

Fig. 6. Functional categorization of brake wear-responsive DEG. A: GO-overrepresentation analysis with the genes that responded to particles from 45 brakings. The 12 GO terms with highest enrichment values were selected. GO analysis was done with panther (Fisher's exact test and Bonferroni correction). B: Expression level of selected genes, displayed as the DESeq2-normalized counts. Significance of DEG was assessed with DESeq2 (lfcThreshold =1, padj $\leq$ 0.05). Asterisks indicate statistical significance (*: $p_{adj} \leq 0.05$; **: $p_{adj} \leq 0.01$; *** $p_{adj} \leq 0.001$; n.s. = not significant).

Additionally, we characterized the elemental character of the ultrafine fractions (16–100 nm) collected with ELPI+ using spICP-MS. This measurement method provides comprehensive information about the number of particles for each element. However, it is not yet possible to determine the composition of individual particles using this technique [31,32]. Thus, we refer to the measured signals as UFP-constituents (UFPC) instead of singular UFP.

Measuring the number of emitted UFPC per braking for each use case, we found that the highway scenario results in the strongest emissions. Regarding elemental compositions, the largest number of UFPC was determined for Fe, followed by Cu, Al, Ti, and Zn. Mo, Ni, and Pb UFPC were about one to three orders of magnitude less abundant (Fig. 1B). This is consistent with published data, which found the elements Fe, Cu, Ti, and Al as major metals in airborne brake wear particles [18,33].

Since the highway-braking scenario led to the highest UFPC concentration in the chamber, we performed all exposure experiments with *A. thaliana* at this use case. Because we also intended to perform background exposures (only the suction flow without brakings), we compared background particle concentration in the chamber with one

highway braking. Particle concentrations at all sizes were several orders of magnitude higher during the highway braking (Fig. S2, C). The observed background concentration is presumably due to the resuspension of sedimented particles by the airflow.

3.2. UFP deposition on leaf surfaces after controlled exposure

First, after exposure to either UFP from 45 highway brakings or to particles from the background exposure, we extracted metallic particles from plant material and measured UFPC with spICP-MS. We found the highest number of UFPC for the metals Fe and Cu. Abundances of Al, Sn, Ti, and Zn were about an order of magnitude lower. Mo, Ni, and Pb were present at comparably low quantities. The elemental constituents of brake dust are strongly dependent on brake pad formulations and data specifically addressing the composition of metallic particles in the ultrafine fraction are lacking. However, especially Fe and Cu are commonly found in high concentrations in brake wear dust and elements such as Ni and Pb are usually less abundant [18]. This suggests that UFP element composition largely reflects the composition of the brake wear material. Apart from small amounts of Fe and Al, we could not detect any UFPC in extracts from background-exposed plants (Fig. 2). In general, we could reliably quantify the extent of UFP deposition and determined satisfactory reproducibility of our exposure experiments (Table S2).

Additionally, the deposition of particles on leaf surfaces was investigated with scanning electron microscopy. We found extensive presence of particles on leaves subjected to brakings, mostly in form of larger agglomerates (Fig. S3). Using transmission electron microscopy, Gonet et al., 2021 also observed agglomeration of brake wear particles and concluded that the larger size fractions mostly comprise agglomerates of UFP [34]. Especially at high concentrations, airborne UFP interact and form agglomerates on the basis of van der Waals- or electrostatic forces, which causes a decrease in the concentration of singular UFP entities [34,35]. Especially weak agglomerates on the basis of van der Waals forces may be abolished by electrostatic impactors such as ELPI+ [36], which is why our measurements (Fig. S2, C) do not allow to comprehensively assess the degree of UFP agglomeration in the chamber.

3.3. Analysis of aerial UFP concentration in the field and particle deposition on leaves

In order to contextualize our results with respect to particle deposition under real life conditions, we performed outdoor exposure experiments with *A. thaliana*. Three locations with varying degrees of traffic volume (rural background; suburban background; inner city) were characterized by collecting UFP with an ELPI+. The highest UFP concentrations were measured at the inner-city location ($\bar{x}_{08:00–18:00}$ = 26,753 UFP*cm3^{-1}) followed by the suburban station ($\bar{x}_{08:00–18:00}$ = 6,540 UFP*cm3^{-1}). The lowest UFP concentrations were measured at the station located in the rural background ($\bar{x}_{08:00–18:00}$ = 4,137 UFP*cm3^{-1}) (Fig. 3, A). Our measurement of the inner-city location is similar to other roadside PNC measurements, as for instance in a street canyon in Manchester, UK, a PNC (4–100 nm) of 27,000 #*cm^{-3} was determined [37,38].

After 2 weeks of outdoor exposure at the three characterized sites, metallic particles were extracted from leaf material and UFP were measured with spICP-MS. We found a consistent pattern of UFPC deposition on leaves with UFPC of all elements displaying the highest concentration on plants from the inner-city location followed by the suburban location and the rural location (Fig. 3, B).

We compared our UFPC quantifications from controlled exposure to the ones from outdoor exposure. Sample assessment with PCA revealed greatest similarity of the inner-city UFPC-profiles to the ones from controlled exposure (Fig. 4, A). For most UFP concentrations we found less than a 10-fold difference between these samples (Fig. 4, B), meaning that the experimental setup leads to an extent of UFP-exposure that lies within a similar order of magnitude as UFP-exposure in the real world. The exception are Cu-UFPC, for which differences much greater than factor 10 were detected throughout (Fig. 4, B, C, D).

For the first time, the approach established here enables investigations into the impact of metallic brake wear-derived non-exhaust emissions on organisms after controlled airborne application of UFPs at a level that is environmentally relevant. Non-exhaust emissions are generally regarded as “woefully understudied” [39] and to date, few studies have attempted to directly analyze the effects of such emissions. Typically, cells or whole organisms are treated with particles suspended in liquids. For example, a recent study on inflammatory responses in macrophages applied brake abrasion dust in such a way [40]. Similarly for plants, available data on brake wear particle toxicity are restricted to the effects of dynamometer-derived particles directly applied to soil (e.g. [41,42]). While these approaches can generate insights into physiological responses, they most likely underrepresent the fraction containing particularly problematic ultrafine particles, do not reflect the natural exposure pathways via air and cannot directly relate the applied particle concentration to real environmental settings.

Thus, the setup introduced in this study opens new experimental perspectives for studies on the toxicity especially of UFPs originating from brake wear. Expanding the focus beyond plants, future studies may yield valuable insights and enhance our understanding regarding the effects of UFP on a diverse range of organisms including mammalian model systems.

3.4. Transcriptomic analysis of A. thaliana after controlled exposure to ultrafine brake dust particles

As a proof of concept and with the aim of gaining first insights into brake-wear induced physiological changes at the molecular level, we performed RNA sequencing with *A. thaliana* rosettes subjected to airborne brake dust UFP. We quantified global gene expression in (i) control plants that were placed next to the exposure chamber, (ii) background exposed plants that were subjected to the airflow of the suction unit, i.e. to residual particles in the pipes of the suction unit and (iii) plants exposed to the airflow of the suction unit with UFP from 45 highway brakings. Rosettes were harvested 24 h after the treatments.

In PCA, we found that both exposures induced similar changes in the transcriptome, since they locate in close proximity but are clearly separated from the controls along PC1 (Fig. 5, C).

Differential expression analysis resulted in 92 differentially expressed genes (DEG) between the background exposure and the control and 150 DEG between the plants subjected to brake wear and the control (Fig. 5, A). In order to address the possible effect of mechanical stress caused by the airflow in the exposure chamber on the transcriptomes of our samples, we investigated the expression patterns of *TCH* genes, which are well established markers for mechanical stress [43]. None of the 4 *TCH* genes was among the DEG, suggesting that neither the background-exposed nor the particle-exposed plants were significantly affected by mechanical stress. The absence of genes encoding heat shock transcription factors (HSFs) or heat shock proteins (HSPs) [44] provides a similar reasoning for heat stress (Supplementary Tables S3 & S4).

Further analysis of the 150 DEG between the controls and the plants subjected to 45 brakings revealed that most of them (134/150) show either a progressive increment or decrement in expression from the controls through the background exposure to the 45 brakings (Fig. 5, B). Our data thus indicate that the background exposure already led to a transcriptional response of many genes that were more strongly affected by the treatment with the wear of 45 brakings. This could indicate a saturating effect, where a lower concentration of UFP triggers similar effects compared to the higher concentration. Moreover, it suggests that plants respond physiologically already to UFP concentrations that are in the range or even below those found at urban traffic sites.

We then functionally categorized UFP-responsive genes. GO

enrichment analysis with the 150 DEG between the brake wear-treated plants and the controls revealed terms related to oxidative stress and various kinds of biotic stress, in particular insect herbivory, and jasmonic acid signaling (Fig. 6 A, Supplementary Table S5). UFP-related elicitation of oxidative stress, for instance through the introduction of redox-active metals. is a proposed mechanism of UFP toxicity in animal tissues [45] and, according to our data, happening in plants, too. Regarding biotic stress, three jasmonate-induced oxygenases (*JOX2*, *JOX3* and *JOX4*) were upregulated under background exposure and to a stronger extent by the treatment with 45 brakings. These changes indicate that the specialized metabolism of plants may be affected by exposure to UFP. Because a large number of specialized metabolites in plants are assumed to function as toxins in herbivore defense [46], the synthesis of potentially harmful compounds could therefore be activated. This calls for systematic monitoring [20], for example through metabolomics studies, to assess possible food safety threats arising from crop plants grown in urban environments.

Also of note, we observed the downregulation of several metal homeostasis genes. The two transcription factor genes *bHLH38* and *bHLH39*, which are involved in Fe homeostasis regulation [47,48] were downregulated by the two treatments. In addition, *COPT2* encoding a copper-transmembrane transporter was found to be downregulated [49, 50] (Fig. 6 B, Supplementary Table S4). The downregulation of these genes suggests that our treatment led to an excess of Fe and Cu within leaves, which had a specific impact on the gene regulatory network that controls the homeostasis of these metals. This interpretation is consistent with the finding that Cu and Fe were the most abundant metals in the UFP released from our brake system (Fig. 2). Considering the composite character of brake wear, which gives rise to a large number of organic compounds [18], the responsiveness of metal homeostasis genes strongly suggests that the metallic constituents within brake wear UFP are contributing to the observed effects at the transcriptomic level. This is in line with the toxicity of metals in ambient particles as observed for exposed animals in previous work [45].

4. Conclusion

This study describes the establishment and validation of a novel approach to study the effects of brake-wear derived UFPs, an important component of non-exhaust emissions, by exposing organisms to airborne particles at environmentally relevant levels. The experimental setup mimics airborne exposure and the UFP-quantifications from field experiments enable an estimation on the real-life proximity of the conducted experiments. Our analysis shows that UFP on inner-city exposed plants are most similar to UFP on plants from the dynamometer exposure as compared to UFP on plants from a rural or suburban location. As a proof of concept, we exposed *A. thaliana* leaves and studied transcriptome responses upon exposure. While some of the identified DEG strongly point towards an influence of metallic particles, the analytical tools used to characterize the exposure conditions only address particle size and elemental composition. Bearing in mind the complexity of brake-wear emissions, a potential plethora of organic molecules may also contribute to the observed alterations in gene expression. Because the amount of UFP on the plants from laboratory exposure and the inner-city are within the same order of magnitude, corresponding effects of UFP on plants in the environment appear probable. Given the complex interplay of various environmental factors that additionally affect plants in the environment, these effects may however still be different from the ones described in our study.

Environmental implication

Even though fine and ultrafine emissions from traffic are among the most relevant pollutants in the environment, their potential effects on flora have received little attention. Toxicity towards plants can be anticipated especially from ultrafine particles (UFP) such as those found in brake wear due to their composition and small diameter. Moreover, deposited UFP could be directly ingested by other organisms and have the potential to alter plant metabolism and thereby modulate the nutritional properties of edible plants. Our study describes the establishment of a setup for exposure of plants to brake wear particles and the resulting transcriptional effects.

Funding

The Bavarian State Ministry of the Environment and Consumer Protection supported this work in the context of the joint research project “BayÖkotox”.

CRediT authorship contribution statement

Ludwig Richtmann: Writing – original draft, Methodology, Investigation, Conceptualization. **Marina Maier:** Writing – review & editing, Methodology, Investigation, Conceptualization. **Thorsten Opel:** Writing – review & editing, Investigation. **Stephan Clemens:** Writing – review & editing, Supervision, Project administration, Funding acquisition, Conceptualization. **Nico Langhof:** Writing – review & editing, Conceptualization.

Declaration of Competing Interest

The authors declare that they have no known competing financial interests or personal relationships that could have appeared to influence the work reported in this paper.

Data availability

Data will be made available on request.

Appendix A. Supporting information

Supplementary data associated with this article can be found in the online version at doi:10.1016/j.jhazmat.2024.134084.

References

[1] Steffen, W., Richardson, K., Rockström, J., Cornell, S.E., Fetzer, I., Bennett, E.M., et al., 2015. Planetary boundaries: guiding human development on a changing planet. Science 347 (6223), 1259855. https://doi.org/10.1126/science.1259855.
[2] Manisalidis, I., Stavropoulou, E., Stavropoulos, A., Bezirtzoglou, E., 2020. Environmental and health impacts of air pollution: a review. Front Public Health 8.
[3] WHO ambient air quality database, 2022 update: status report. ⟨https://www.who.int/publications-detail-redirect/9789240047693⟩ (Accessed 2023–08-16).
[4] Molina Rueda, E., Carter, E., L'Orange, C., Quinn, C., Volckens, J., 2023. Size-resolved field performance of low-cost sensors for particulate matter air pollution. Environ Sci Technol Lett 10 (3), 247–253. https://doi.org/10.1021/acs.estlett.3c00030.
[5] Saha, P.K., Zimmerman, N., Malings, C., Hauryliuk, A., Li, Z., Snell, L., et al., 2019. Quantifying high-resolution spatial variations and local source impacts of urban ultrafine particle concentrations. Sci Total Environ 655, 473–481. https://doi.org/10.1016/j.scitotenv.2018.11.197.
[6] Zhang, K., Wang, D., Bian, Q., Duan, Y., Zhao, M., Fei, D., et al., 2017. Tethered balloon-based particle number concentration, and size distribution vertical profiles within the lower troposphere of shanghai. Atmos Environ 154, 141–150. https://doi.org/10.1016/j.atmosenv.2017.01.025.
[7] Kwon, H.-S., Ryu, M.H., Carlsten, C., 2020. Ultrafine particles: unique physicochemical properties relevant to health and disease. Exp Mol Med 52 (3), 318–328. https://doi.org/10.1038/s12276-020-0405-1.
[8] Sun, J., Birmili, W., Hermann, M., Tuch, T., Weinhold, K., Merkel, M., et al., 2020. Decreasing trends of particle number and black carbon mass concentrations at 16 observational sites in Germany from 2009 to 2018. Atmos Chem Phys 20 (11), 7049–7068. https://doi.org/10.5194/acp-20-7049-2020.
[9] Moreno-Ríos, A.L., Tejeda-Benítez, L.P., Bustillo-Lecompte, C.F., 2022. Sources, characteristics, toxicity, and control of ultrafine particles: an overview. Geosci Front 13 (1), 101147. https://doi.org/10.1016/j.gsf.2021.101147.
[10] Beddows, D.C.S., Harrison, R.M., Gonet, T., Maher, B.A., Odling, N., 2023. Measurement of road traffic brake and tyre dust emissions using both particle composition and size distribution data. Environ Pollut 331, 121830. https://doi.org/10.1016/j.envpol.2023.121830.

[11] Harrison, R.M., Jones, A.M., Gietl, J., Yin, J., Green, D.C., 2012. Estimation of the contributions of brake dust, tire wear, and resuspension to nonexhaust traffic particles derived from atmospheric measurements. Environ Sci Technol 46 (12), 6523–6529. https://doi.org/10.1021/es300894r.
[12] Hong, G., Jee, Y.-K., 2020. Special issue on ultrafine particles: where are they from and how do they affect us? Exp Mol Med 52 (3), 309–310. https://doi.org/10.1038/s12276-020-0395-z.
[13] Chang, C.-Y., You, R., Armstrong, D., Bandi, A., Cheng, Y.-T., Burkhardt, P.M., et al., 2022. Chronic exposure to carbon black ultrafine particles reprograms macrophage metabolism and accelerates lung cancer. Sci Adv 8 (46), eabq0615. https://doi.org/10.1126/sciadv.abq0615.
[14] Lin, S., Ryan, I., Paul, S., Deng, X., Zhang, W., Luo, G., et al., 2022. Particle surface area, ultrafine particle number concentration, and cardiovascular hospitalizations. Environ Pollut 310, 119795. https://doi.org/10.1016/j.envpol.2022.119795.
[15] Clemens, S., 2006. Toxic metal accumulation, responses to exposure and mechanisms of tolerance in plants. Biochimie 88 (11), 1707–1719. https://doi.org/10.1016/j.biochi.2006.07.003.
[16] El-Shetehy, M., Moradi, A., Maceroni, M., Reinhardt, D., Petri-Fink, A., Rothen-Rutishauser, B., et al., 2021. Silica nanoparticles enhance disease resistance in arabidopsis plants. Nat Nanotechnol 16 (3), 344–353. https://doi.org/10.1038/s41565-020-00812-0.
[17] Wang, W.-N., Tarafdar, J.C., Biswas, P., 2013. Nanoparticle synthesis and delivery by an aerosol route for watermelon plant foliar uptake. J Nanopart Res 15 (1), 1417. https://doi.org/10.1007/s11051-013-1417-8.
[18] Grigoratos, T., Martini, G., 2015. Brake wear particle emissions: a review. Environ Sci Pollut Res 22 (4), 2491–2504. https://doi.org/10.1007/s11356-014-3696-8.
[19] Clemens, S., Ma, J.F., 2016. Toxic heavy metal and metalloid accumulation in crop plants and foods. Annu Rev Plant Biol 67 (1), 489–512. https://doi.org/10.1146/annurev-arplant-043015-112301.
[20] Meharg, A.A., 2016. Perspective: city farming needs monitoring. S60–S60 Nature 531 (7594). https://doi.org/10.1038/531S60a.
[21] Alonso, J.M., Stepanova, A.N., Leisse, T.J., Kim, C.J., Chen, H., Shinn, P., et al., 2003. Genome-wide insertional mutagenesis of Arabidopsis thaliana. Science 301 (5633), 653–657. https://doi.org/10.1126/science.1086391.
[22] Laughton, S., Laycock, A., Bland, G., von der Kammer, F., Hofmann, T., Casman, E. A., et al., 2021. Methanol-based extraction protocol for insoluble and moderately water-soluble nanoparticles in plants to enable characterization by single particle ICP-MS. Anal Bioanal Chem 413 (2), 299–314. https://doi.org/10.1007/s00216-020-03014-8.
[23] Montaño, M.D., Olesik, J.W., Barber, A.G., Challis, K., Ranville, J.F., 2016. Single particle ICP-MS: advances toward routine analysis of nanomaterials. Anal Bioanal Chem 408 (19), 5053–5074. https://doi.org/10.1007/s00216-016-9676-8.
[24] Shimamura, Y.; Hsu, D.; Yamanaka, M. Multielement Nanoparticle Analysis of Semiconductor Process Chemicals Using spICP-QQQ.
[25] Laborda, F., Gimenez-Ingalaturre, A.C., Bolea, E., Castillo, J.R., 2019. Single particle inductively coupled plasma mass spectrometry as screening tool for detection of particles. Spectrochim Acta Part B Spectrosc 159, 105654. https://doi.org/10.1016/j.sab.2019.105654.
[26] Nazar, M.F., Shah, S.S., Eastoe, J., Khan, A.M., Shah, A., 2011. Separation and recycling of nanoparticles using cloud point extraction with non-ionic surfactant mixtures. J Colloid Interface Sci 363 (2), 490–496. https://doi.org/10.1016/j.jcis.2011.07.070.
[27] Pischke, E., Barozzi, F., Colina Blanco, A.E., Kerl, C.F., Planer-Friedrich, B., Clemens, S., 2022. Dimethylmonothioarsenate is highly toxic for plants and readily translocated to shoots. Environ Sci Technol 56 (14), 10072–10083. https://doi.org/10.1021/acs.est.2c01206.
[28] Love, M.I., Huber, W., Anders, S., 2014. Moderated estimation of fold change and dispersion for RNA-seq data with DESeq2. Genome Biol 15 (12), 550. https://doi.org/10.1186/s13059-014-0550-8.
[29] Sinha, A., Ischia, G., Menapace, C., Gialanella, S., 2020. Experimental characterization protocols for wear products from disc brake materials. Atmosphere 11 (10), 1102. https://doi.org/10.3390/atmos11101102.
[30] Mathissen, M., Scheer, V., Vogt, R., Benter, T., 2011. Investigation on the potential generation of ultrafine particles from the tire–road interface. Atmos Environ 45 (34), 6172–6179. https://doi.org/10.1016/j.atmosenv.2011.08.032.
[31] Yamanaka, M.; Itagaki, T.; Wilbur, S. Acquire NP Data for up to 16 Elements in Rapid Multi-Element Nanoparticle Analysis Mode.
[32] Soffey, E., Jones, C., Kelinske, M., 2019. Rapid multielement nanoparticle analysis using single-particle ICP-MS/MS. Spectroscopy 34 (5), 10–20.
[33] Wahlström, J., Olander, L., Olofsson, U., 2010. Size, shape, and elemental composition of airborne wear particles from disc brake materials. Tribol Lett 38 (1), 15–24. https://doi.org/10.1007/s11249-009-9564-x.
[34] Gonet, T., Maher, B.A., Nyirő-Kósa, I., Pósfai, M., Vaculík, M., Kukutschová, J., 2021. Size-resolved, quantitative evaluation of the magnetic mineralogy of airborne brake-wear particulate emissions. Environ Pollut 288, 117808. https://doi.org/10.1016/j.envpol.2021.117808.
[35] Bruinink, A., Wang, J., Wick, P., 2015. Effect of particle agglomeration in nanotoxicology. Arch Toxicol 89 (5), 659–675. https://doi.org/10.1007/s00204-015-1460-6.
[36] Kero, I., Naess, M.K., Tranell, G., 2015. Particle size distributions of particulate emissions from the ferroalloy industry evaluated by electrical low pressure impactor (ELPI). J Occup Environ Hyg 12 (1), 37–44. https://doi.org/10.1080/15459624.2014.935783.
[37] Longley, I.D., Gallagher, M.W., Dorsey, J.R., Flynn, M., Allan, J.D., Alfarra, M.R., et al., 2003. A case study of aerosol (4.6nm). Atmos Environ 37 (12), 1563–1571. https://doi.org/10.1016/S1352-2310(03)00010-4.
[38] Kumar, P., Morawska, L., Birmili, W., Paasonen, P., Hu, M., Kulmala, M., et al., 2014. Ultrafine particles in cities. Environ Int 66, 1–10. https://doi.org/10.1016/j.envint.2014.01.013.
[39] Fussell, J.C., Franklin, M., Green, D.C., Gustafsson, M., Harrison, R.M., Hicks, W., et al., 2022. A review of road traffic-derived non-exhaust particles: emissions, physicochemical characteristics, health risks, and mitigation measures. Environ Sci Technol 56 (11), 6813–6835. https://doi.org/10.1021/acs.est.2c01072.
[40] Selley, L., Schuster, L., Marbach, H., Forsthuber, T., Forbes, B., Gant, T.W., et al., 2020. Brake dust exposure exacerbates inflammation and transiently compromises phagocytosis in macrophages. Metallomics 12 (3), 371–386. https://doi.org/10.1039/C9MT00253G.
[41] Piacentini, D., Falasca, G., Canepari, S., Massimi, L., 2019. Potential of PM-selected components to induce oxidative stress and root system alteration in a plant model organism. Environ Int 132, 105094. https://doi.org/10.1016/j.envint.2019.105094.
[42] Maiorana, S., Teoldi, F., Silvani, S., Mancini, A., Sanguineti, A., Mariani, F., et al., 2019. Phytotoxicity of wear debris from traditional and innovative brake pads. Environ Int 123, 156–163. https://doi.org/10.1016/j.envint.2018.11.057.
[43] Braam, J., Davis, R.W., 1990. Rain-, wind-, and touch-induced expression of calmodulin and calmodulin-related genes in arabidopsis. Cell 60 (3), 357–364. https://doi.org/10.1016/0092-8674(90)90587-5.
[44] Haider, S., Raza, A., Iqbal, J., Shaukat, M., Mahmood, T., 2022. Analyzing the regulatory role of heat shock transcription factors in plant heat stress tolerance: a brief appraisal. Mol Biol Rep 49 (6), 5771–5785. https://doi.org/10.1007/s11033-022-07190-x.
[45] Kelly, F.J., Fussell, J.C., 2012. Size, source and chemical composition as determinants of toxicity attributable to ambient particulate matter. Atmos Environ 60, 504–526. https://doi.org/10.1016/j.atmosenv.2012.06.039.
[46] Erb, M., Reymond, P., 2019. Molecular interactions between plants and insect herbivores. Annu Rev Plant Biol 70 (1), 527–557. https://doi.org/10.1146/annurev-arplant-050718-095910.
[47] Yuan, Y., Wu, H., Wang, N., Li, J., Zhao, W., Du, J., et al., 2008. FIT interacts with AtbHLH38 and AtbHLH39 in regulating iron uptake gene expression for iron homeostasis in Arabidopsis. Cell Res 18 (3), 385–397. https://doi.org/10.1038/cr.2008.26.
[48] Wang, N., Cui, Y., Liu, Y., Fan, H., Du, J., Huang, Z., et al., 2013. Requirement and functional redundancy of ib subgroup bHLH proteins for iron deficiency responses and uptake in Arabidopsis thaliana. Mol Plant 6 (2), 503–513. https://doi.org/10.1093/mp/sss089.
[49] Bernal, M., Casero, D., Singh, V., Wilson, G.T., Grande, A., Yang, H., et al., 2012. Transcriptome sequencing identifies SPL7-regulated copper acquisition genes FRO4/FRO5 and the copper dependence of iron homeostasis in Arabidopsis. Plant Cell 24 (2), 738–761. https://doi.org/10.1105/tpc.111.090431.
[50] Cai, Y., Li, Y., Liang, G., 2021. FIT and bHLH Ib transcription factors modulate iron and copper crosstalk in Arabidopsis. Plant Cell Environ 44 (5), 1679–1691. https://doi.org/10.1111/pce.14000.